The probability of chromatin to be at the nuclear lamina has no systematic effect on its transcription level

Yoonjin Kim[1,†], **Alexander Y. Afanasyev**[2,†], **Igor S. Tolokh**[1], **Igor V. Sharakhov**[3,*], **Alexey V. Onufriev**[1,4,5,*]

***For correspondence:**
alexey@cs.vt.edu (AO); igor@vt.edu (IS)

[†]These authors contributed equally to this work

[1]Department of Computer Science, Virginia Tech, Blacksburg, VA 24061, USA; [2]Department of Biomedical Engineering and Mechanics, Virginia Tech, Blacksburg, VA 24061, USA; [3]Department of Entomology, Virginia Tech, Blacksburg, VA 24061, USA; [4]Department of Physics, Virginia Tech, Blacksburg, VA 24061, USA; [5]Center for Soft Matter and Biological Physics, Virginia Tech, Blacksburg, VA 24061, USA

Abstract

Multiple studies have shown a correlation between gene expression and positioning of genes at nuclear envelope (NE) lined by nuclear lamina. Here, we ask whether there is a causal, systematic connection between the expression level of the groups of genes in topologically associating domains (TADs) of Drosophila nuclei and the probability of TADs to be found at the NE. To investigate the connection, we combine a coarse-grained dynamic model of the entire Drosophila nucleus with the genome-wide gene expression data for both the control and lamins depleted (LD) nuclei. We analyze the TAD averaged transcription levels of genes against the probabilities of individual TADs to be near the NE. Our findings suggest that, within statistical error margin, positioning of Drosophila TADs at the nuclear envelope does not, by itself, systematically affect the average gene expression in these TADs, while the expected negative correlation is confirmed. Verifiable hypotheses of the underlying mechanism for the presence of correlation without causality are discussed.

We introduce a TAD length normalized metric for the average transcription activity of genes in a TAD: number of Reads mapped to all genes in a TAD Per Kilobase of TAD length per Million reads mapped to all TADs (RPKMT).

Introduction

The nucleus in the eukaryotic cells is separated from the cytoplasm by the nuclear envelope (NE), the internal surface of which is lined by the nuclear lamina (NL) - a meshwork of lamins and associated proteins ***Buchwalter et al.*** (***2018***); ***Briand and Collas*** (***2020***). Lamins, as the major structural proteins of the NL, are considered to be an important determinant of nuclear architecture and gene expression ***Briand and Collas*** (***2020***). Multiple studies have shown a correlation between positioning at the NL/NE and repression of transgenes and some endogenous genes ***Dietzel et al.*** (***2004***); ***Misteli*** (***2007***); ***Kosak et al.*** (***2002***); ***Hewitt et al.*** (***2004***); ***Zink et al.*** (***2004***); ***Williams et al.*** (***2006***). Genes that move away from the nuclear periphery, either in lamin mutants (LM) or during tissue differentiation, have been shown to be transcriptionally upregulated ***Williams et al.*** (***2006***); ***Chuang et al.***

(*2006*); *Malhas et al.* (*2007*). However, expression of other genes appears unaffected by their proximity to the nuclear periphery *Nielsen et al.* (*2002*); *Zhou et al.* (*2002*); *Hewitt et al.* (*2004*). Several studies directly tested functional consequences of chromatin-lamina association by tethering individual genes to the nuclear periphery in human cells using the lacO/LacI system *Finlan et al.* (*2008*); *Kumaran and Spector* (*2008*); *Reddy et al.* (*2008*). Since binding of nucleoplasmic LacI molecules to lacO sites in the reporter construct did not, by itself, impair transcription *Finlan et al.* (*2008*); *Reddy et al.* (*2008*), these studies provided direct evidence for a causative role of the nuclear periphery in altering gene expression of many genes. For example, 51 endogenous genes located around a site of NE-attachment have been repressed, suggesting that an inactive chromosomal domain has been generated upon tethering to the lamina *Reddy et al.* (*2008*). Importantly, the transcriptional repression caused by tethering of a gene to the NE was accompanied by histone H4 hypoacetylation, implying the importance of epigenetic modifications in this process, not necessarily the geometric proximity to the NE *per se*. At the same time, some tethered genes were not repressed *Finlan et al.* (*2008*); *Reddy et al.* (*2008*). Moreover, other experiments have demonstrated that lamina-targeted genetic loci can still be activated and transcribed at the lamina *Kumaran and Spector* (*2008*).

The tethering studies suggest that, for some genes, the NL represents a repressive compartment in the cell nucleus, but the repression can be overcome by other genes. Overall, these works discovered important features of individual genes and groups of genes, but they did not make genome-wide conclusions. Thus, we are still lacking a statistically significant conclusion on possible causative relationship between proximity to the NE/NL and gene expression. Moreover, chromosome loci in the interphase nuclei are known to be highly mobile *Csink and Henikoff* (*1998*); *Chubb et al.* (*2002*); *Spector* (*2003*); *Lanctôt et al.* (*2007*), therefore, experiments in which a locus is permanently anchored to the NE may not represent the highly mobile nature of chromatin. An experiment which directly probes a casual connection between expression of a gene and its necessarily stochastic position relative to the NE would be most appropriate, but to the best of our knowledge, no such studies have been performed on genome-wide scale. The difficulties in performing this kind of analysis purely experimentally motivate combining experiment with an appropriate computer modeling to make progress. Here, experiment can provide gene expression data, while computer modeling can trace the movement of the relevant chromatin units with the desired spatial and temporal resolution on genome-wide scale to detect systematic trends, if any. Due to the highly stochastic nature of transcription at the level of individual genes, an appropriate unit of chromatin structure beyond individual genes is desirable to explore systematic trends in gene expression.

Application of the chromosome conformation capture technique with high-throughput sequencing (Hi-C) to study chromatin organization identified topologically associating domains (TADs) in various organisms of high eukaryotes *Lieberman-Aiden et al.* (*2009*); *Dixon et al.* (*2012*); *Nora et al.* (*2012*); *Sexton et al.* (*2012*); *Ulianov et al.* (*2015*). TADs may contain multiple genes, range in size from tens of kilobases (kb) in fruit fly to several megabases (Mb) in mammals, and represent structural and functional units of three-dimensional (3D) chromatin organization *Sexton and Cavalli* (*2015*); *Gorkin et al.* (*2014*); *Rowley and Corces* (*2018*); *Yasuhara and Zou* (*2021*). Since the boundaries between TADs are conserved among cell types and sometimes across species *Dixon et al.* (*2012*); *Phillips-Cremins et al.* (*2013*); *Rao et al.* (*2014*); *Dixon et al.* (*2015*); *Acemel et al.* (*2017*); *Ulianov et al.* (*2021*); *Renschler et al.* (*2019*); *Torosin et al.* (*2020*); *Liao et al.* (*2021*), TADs can be regarded as stable structural units of chromatin, making TAD a natural unit of genome partitioning for exploring systematic structure-function relationships in chromatin. Certain TADs overlap with chromatin regions, called lamina-associated chromatin domains or LADs, that have been systematically identified using a DamID approach in humans and fruit flies *Guelen et al.* (*2008*); *van Bemmel et al.* (*2010*); *Pindyurin et al.* (*2018*). Although a small fraction of genes located in LADs can express (about 10%), transcription of the majority of genes inside LADs is repressed *Pickersgill et al.* (*2006*); *Guelen et al.* (*2008*); *van Bemmel et al.* (*2010*); *Ulianov et al.* (*2019*); *Zheng et al.*

(*2015*); *Wu and Yao* (*2017*). Only about 25-30% of all LADs are located at the nuclear periphery at any given moment in any given Drosophila cell *Pickersgill et al.* (*2006*); *Guelen et al.* (*2008*); *van Bemmel et al.* (*2010*); *Ulianov et al.* (*2019*). Moreover, as was recently discovered, LADs in fruit fly, despite having relatively strong affinity to the NE, can still be highly mobile within each nucleus *Tolokh et al.* (*2022*), with most LADs coming in contact with the NE and moving away from it multiple times during the interphase. Thus, experiments that permanently attach a LAD to the NE may not be ideal to mimic *in vivo* reality with respect to possible effects of the NE on transcription of genes in fruit fly LADs.

Here, we combine prior genome-wide transcription analysis *Ulianov et al.* (*2019*) with a novel modeling approach to test the functional role of the TAD proximity to the NE in the *Drosophila* genome, taking into account its mobile nature over the interphase. For this purpose, we employ a recently developed model of the fruit fly interphase chromatin *Tolokh et al.* (*2022*) that describes dynamics and spatial organization of the entire diploid set of chromosomes, and their interactions with the NE, at TAD-resolution. The model, which takes into account different epigenetic classes of TADs, TAD-TAD contact probabilities (Hi-C map) and the known distribution of LADs along the genome, reproduces experimentally observed chromatin density profiles for both control and lamins depleted (LD) nuclei and can faithfully predict the probabilities of individual TADs to be in the layer adjacent to the NE.

To estimate mRNA abundance from RNA sequencing (RNA-seq) data, a number of metrics have been proposed such as RPKM (reads per kilobase of transcript per million reads mapped), FPKM (fragments per kilobase of transcript per million fragments mapped) or TPM (transcripts per million), to name a few. To investigate the genome-wide relationship between positioning of TADs at the NE and gene transcription at TAD resolution, a relevant metric of transcription activity is required – to the best of our knowledge, no such TAD-focused metric is currently available, and one will be proposed here.

Results

TAD transcription levels and the probability of a TAD to be near the NE: correlation.

It has been suggested previously that the chromatin near the NE may be in a transcription suppressing environment *Shachar and Misteli* (*2017*). Here we investigate whether transcription levels of TADs, which are relatively free to move within a nucleus during the interphase, correlate with their geometric proximity to the NE. Should such a correlation be found, perhaps for a subgroup of TADs, we would like to test whether the positioning of TADs at the NE *per se* causes the change in transcription.

To this end, we need a probabilistic metric for TAD-NE proximity, because the same TAD can move in and out of a proximity to the NE multiple times during the interphase *Tolokh et al.* (*2022*). It is reasonable to assume that, if a proximity to the NE suppresses transcription, the degree of suppression of a TAD transcription activity should be related to the fraction of time the TAD spends in a proximity to (in contact with) the NE. This fraction can be expressed as the probability of a TAD to be in the very narrow contact layer near the NE, that is, when its center is within 0.2 μm (average bead diameter) from the NE, see Materials and Methods. We consider this probability (frequency) of a TAD to be in this layer near the NE, that is to be essentially in contact with the NE, as a suitable measure of the TAD's *stochastic* proximity to the NE.

We also propose a normalized metric for gene transcription levels at TAD resolution, RPKMT (number of Reads mapped to all genes in a TAD per Kilobase of TAD length per Million reads mapped to all TADs). This metric considers each TAD as one transcription unit instead of a gene, as RPKM does, and normalizes the transcription reads in each TAD using the whole DNA length of a TAD, see Materials and Methods. Such a normalization eliminates the effects of gene overlaps in TADs and makes estimating the transcription activities of genes in a TAD more simple and robust.

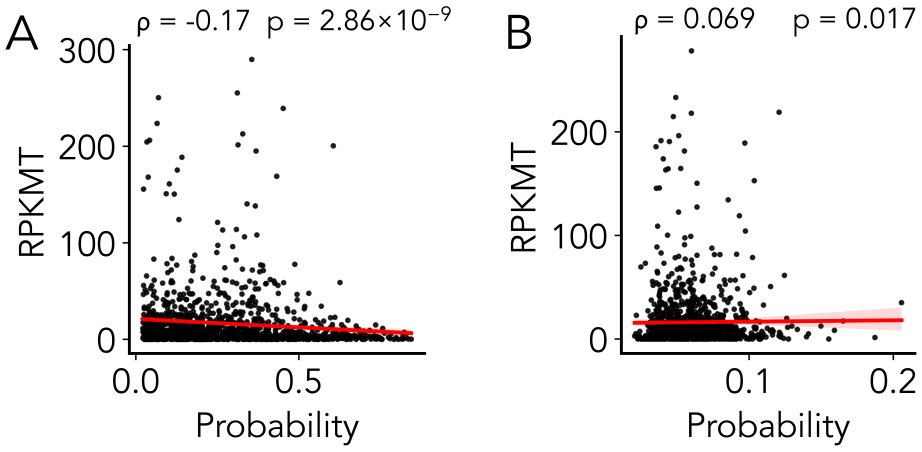

Figure 1. (A) Scatter plot showing a weak negative correlation between the TAD expression (in RPKMT) and the probability of TAD to be found in contact with the NE (i.e. to be found within 0.2 μm layer near the NE) in the control nuclei. **(B)** Scatter plot showing no correlation between the TAD expression (in RPKMT) and the probability of TAD to be found in contact with the NE in the lamins depleted (LD) nuclei. The Spearman correlation coefficients (ρ), p-values (n=1169, two-tailed Student's t-test with *(n-2)* degrees of freedom), and linear regression lines (red; 95% confidence intervals in pink) are shown. Statistical significance is defined as $p < 0.05$. Plots are generated with the *lmplot* function in Seaborn.

As seen from Figure 1A, there is a weak negative correlation between the transcription activity of TADs (RPKMT) and their probability to be in contact with the NE in the control *Drosophila* nuclei. The absence of a pronounced negative correlation may be unexpected, as transcription in LADs and, therefore, in LAD containing TADs (L-TADs), which are NE-bound, is well known to be suppressed ***Kim et al.*** (***2019***); ***Briand and Collas*** (***2020***); ***van Bemmel et al.*** (***2010***), and the fraction of L-TADs in *Drosophila*, ≈30%, is significant ***Sexton et al.*** (***2012***). Not surprisingly, Figure 1B shows essentially no correlation between the transcription activities of TADs (RPKMT) and their probabilities to be in contact with the NE in LD nuclei.

To investigate the findings further, we have analyzed the transcription *vs.* probability to be in contact with the NE for TADs containing LADs (L-TADs) and for TADs not containing LADs (nonL-TADs) separately. To help discern meaningful, systematic genome-wide trends behind large natural variation of transcription activity between individual TADs, we have binned the data, based on the probability of each TAD to be in contact with the NE, as shown in Fig. 2 – each bin contains an equal number of TADs (see Materials and Methods), the height of the bar indicates the average transcription level of the TADs in this bin. Considering all TAD types together, Fig. 2 (A), the TADs in the rightmost bin # 6 – TADs that are most likely to be in contact with the NE most of the time – do show a marked decrease in transcription, but the trend does not continue for TADs that are still likely to be in contact with the NE, *e.g.*, the height of bin # 5 is the same as that of the leftmost bin # 1, which corresponds to TADs that are almost never in contact with the NE. We have hypothesized that the abrupt drop in transcription seen in bin # 6 is due to TADs containing LADs. The hypothesis is confirmed in Fig. 2 (C), from which TADs containing LADs have been excluded: no correlation with the likelihood to be in contact with the NE is seen (the drop seen in bin # 4 is irrelevant to this conclusion, and will be discussed below).

In summary, our first conclusion is that the weak negative correlation between transcription level of a TAD and its stochastic proximity to the NE in the control cells is due to only those TADs that contain LADs, that is L-TADs. Otherwise, there is no correlation. Consistent with this conclusion is a clear "ladder" of gradually diminishing transcription levels of TADs containing LADs as the stochastic proximity to the NE increases, Fig. 2 (E). A hypothesis on why the transcription activity of TADs containing LADs in Fig. 2 still shows a clear correlation "ladder" is presented in the

first paragraph of "Ideas and Speculations." Note that the transcription activity of L-TADs is about five times lower than that of nonL-TADs ***Ulianov et al.*** (***2019***), which explains both the very weak genome-wide negative correlation seen in Fig. 1 (A), and the fact that no negative correlation with the proximity to the NE is seen for all TADs in Fig. 2 (A), if one excludes the rightmost bin composed almost exclusively of L-TADs, see Fig. 2 (C).

Going back to the clear "ladder" of decreasing transcription level with the stochastic proximity to the NE, the only exception is the leftmost bin # 1 in Fig. 2 (E), which corresponds to the low probability of ~ 0.2 to be in contact with the NE. This is the same exception as seen in other bins, corresponding to the same ~ 0.2 probability of being in contact with the NE. We argue that this drop in transcription seen for a certain subset of specific TADs that rarely come in contact with the NE – the TADs in bin # 3 in Fig. 2 (A), TADs in bin # 4 and bin # 3 in Fig. 2 (C) or the leftmost bin #1 in Fig. 2 (E) – is irrelevant to the arguments made above. This is because the drop is there for L-TADs and nonL-TADs alike, and it stays unchanged despite the major re-arrangement of the chromatin in lamins depleted cells, open bars in Fig. 2 (see also Fig. 1 in Appendix 2). We hypothesize that the explanation for why this subset of TADs shows depressed transcription may have to do with their epigenetic composition distinctly different from other TADs, see Fig. 1 in Appendix 1. Since the issue is tangential to the main question of this paper, we do not pursue it further in this work.

TAD transcription levels and the probability of a TAD to be near the NE: causation.

A natural question arises whether the clear negative correlation of transcription activity of L-TADs with their stochastic proximity to the NE is causal, that is whether the increased probability to find a TAD in contact with the NE, by itself, causes the transcription level to decrease?

To this end, we have considered the transcription patterns in lamins depleted cells. First, note that the lamins knockdown causes a drastic spatial re-arrangement of chromatin within the nucleus ***Ulianov et al.*** (***2019***) – most of TADs move away from the NE, Fig. 2 (B,D,F), as well as Fig. 1 in Appendix 2. In fact, the probability to find most of the TADs in contact with the NE in lamins depleted nuclei is less than 0.1, with no bins extending beyond 0.2, Fig. 2 (B). See also Fig. 2 in Appendix 1 for the stark contrast between the control and lamins depleted cells in this respect. So, if being in contact with the NE with an appreciable probability caused the transcription in TADs containing LADs to drop, the transcriptional activity would be expected to recover almost fully in lamins depleted nuclei. Yet no change in transcription levels are seen in the *same* groups of TADs, Fig. 2, open bars. Note that we deliberately kept exactly the same TADs in each lamins depleted bin as in the control.

Thus, our second and main conclusion is that stochastic proximity to the NE of TADs, which are highly mobile, does not, by itself, cause a noticeable *systematic, genome-wide* change in transcription at TAD resolution.

Discussion

This work has combined simulation and experiment to arrive at the following result: the probability of a TAD to be found in contact with the NE, by itself, has no systematic, causal effect on its transcription level in *Drosophila*. We stress several key aspects of this statement. First, it applies to a systematic trend only, averaged across multiple TADs. As shown recently ***Ulianov et al.*** (***2019***), it is entirely possible for transcription levels of a subset of individual, weakly expressing TADs to increase in lamins depleted nuclei, where their probability to be in contact with the NE is expected to decrease relative to the control nuclei. There is no contradiction here with our main claim: even if more TADs become transcriptionally up-regulated then down-regulated upon lamins depletion, which was seen in Ref. ***Ulianov et al.*** (***2019***), the net effect averaged over large groups of TADs can still be zero. And this what we are finding, within the statistical margin of error. In addition, lamins knockdown used in Ref. ***Ulianov et al.*** (***2019***) can affect gene expression in more than one way,

including increasing of the acetylation level at histone H3 and decreasing chromatin compaction in LADs.

Second, we stress the highly mobile nature of TADs **Tolokh et al.** (**2022**), including L-TADs, reflected in our deliberate word choice of "probability to be in contact with the NE" *vs.* more common "proximity to the NE". L-TADs, even those that are likely to be found in contact with the NE, move away from the NE multiple times during the interphase **Tolokh et al.** (**2022**). Thus, the condition of a stable attachment to the NE, *e.g., via* a tether, is not reproduced in live *Drosophila* nuclei, which removes the potential contradiction with the pioneering tethering studies that demonstrated down-regulation of certain loci upon induced contact with the NE **Finlan et al.** (**2008**); **Kumaran and Spector** (**2008**); **Reddy et al.** (**2008**). Indeed, targeting of lamin-associated loci does not take place during interphase when loci can only form transient contacts with the lamina **Kumaran and Spector** (**2008**). Stable tethering of a locus to the nuclear lamina requires passage through mitosis. Similarly, treatment of *Drosophila* S2 cells with dsRNA against lamin Dm0 was performed over four days **Ulianov et al.** (**2019**) allowing passages through mitosis. It is likely that cell division is necessary for re-setting of an epigenetic state of the chromatin at the nuclear periphery. Thus, epigenetic marks and transcription levels of TADs are unlikely to change during the same interphase, despite the fact that TADs frequently change theirs positions with respect to the lamina.

Different mechanisms for LAD positioning and repression are not expected to be mutually exclusive. A recent study performed a detailed analysis of gene repression mechanisms in LADs using human K562 cells **Leemans et al.** (**2019**). By systematically moving promoters from their native LAD location to a more neutral chromatin environment and by transplanting them to a wide range of chromatin contexts inside LADs, the study has demonstrated that the variation in the expression level can be due to the interplay between promoter sequence and local chromatin features in the LADs **Leemans et al.** (**2019**). Chromatin features in the LADs can be partially responsible for interaction with the lamina since lowering H3K9me2/3 levels decreases LAD-contacts in human cells **Kind et al.** (**2013**, 2015). Thus, the lamina can attract loci of inactive chromatin contributing to the assembly of repressive peripheral chromatin domains. The NE proteins can also attract chromatin to the lamina and participate in repression of transcription. For example, histone deacetylase HDAC3, which is associated with the NE transmembrane (NET) protein Lap2beta and the DNA-binding protein cKrox, was shown to attract LADs to the nuclear periphery in mice cells **Zullo et al.** (**2012**); **Poleshko et al.** (**2017**) and Drosophila S2 cells **Milon et al.** (**2012**). Inhibition of histone deacetylation with trichostatin A (TSA) in *Drosophila* cells causes loss of Lamin binding to chromatin **Pickersgill et al.** (**2006**). Thus, nuclear lamina-associated HDACs could contribute to the repressive environment of the nuclear periphery by down regulating gene expression **Somech et al.** (**2005**); **Demmerle et al.** (**2013**) and assembling the peripheral chromatin. Moreover, lamins themselves can affect both position and transcription of chromatin. A study has shown that artificial anchoring of lamins to promoters of transfected reporter plasmids can lead to reduced transcription **Lee et al.** (**2009**). A conditional and temporal up-regulation of lamin C in *Drosophila* caused a shift in chromatin distribution from peripheral to central, which was associated with reduced levels of the active chromatin mark H3K9ac **Amiad-Pavlov et al.** (**2021**). Depletion of lamin Dm0 resulted in the moderate upregulation of the generally very weak background transcription in LADs but not in the inter-LADs in *Drosophila* S2 cells **Ulianov et al.** (**2019**). Similarly, lamin B1 depletion decreased heterochromatin marker H3K27me3 was drastically reduced by 80 percent in human cells **Stephens et al.** (**2018**).

Our study has several limitations. The conclusions rely on predictions of a computational model: while the systematic, and even a few individual, trends in the predicted TAD positioning have been verified against experiment, deviations from reality may still occur on the level of individual TADs. Thus, we stress the systematic nature of the main conclusions, likely correct in the average sense. A related limitation is that the minimal structural unit of chromatin employed in this work is TAD, which is about 100 kb for *Drosophila*. We do not make any claims for what might be happening at finer resolutions, including promoter-enhancer interactions withing TADs. The cell types used to

define the epigenetic classes employed by the computational model and to generate the transcription profiles (RNA-seq) were taken from related but not exactly the same cell cultures. The concern is mitigated by the fact that both cell types have embryonic origin. Moreover, we have confirmed the consistency of the transcription profiles within the four epigenetic classes of TADs between S2 embryonic cell line data ***Ulianov et al.*** (***2019***) used in our study, Fig. 3 (left panel), and 16-18 hr embryos data ***Sexton et al.*** (***2012***) presented in Fig. 3 (right panel). The data from this latter work (***Sexton et al.*** (***2012***)) were used to develop parameters of the computer model ***Tolokh et al.*** (***2022***) which we use to compute the TAD-NE contact probablities.

The third limitation is that the lamin knockdown may not only cause global chromatin relocation, but also epigenetic perturbation of TADs. This concern is mitigated by the fact that the level of histone H3 acetylation is elevated only in LADs, but not in the LAD-free regions upon Lamin knockdown when compared to control cells ***Ulianov et al.*** (***2019***). Thus, the epigenetic profiles of the majority of TADs is expected to be unchanged upon the Lamin knockdown.

Ideas and Speculations

The main implication of this work is that, with some relatively rare exceptions, the role of the NE does not include significant systematic regulation of transcription states of genes in TADs. Instead, the lamina may help to "lock in" the repression state by more than one mechanism. First, the nuclear lamina may facilitate a better separation of active and inactive chromatin by sequestering inactive TADs (Null, PcG and HP1) at the nuclear periphery. This can be achieved by yet unknown mechanism of attraction between the NE proteins and specific histone modification and/or chromatin proteins. In this mechanism, the epigenetic profile of TADs determines both their affinity to the NE and transcriptional repression. That would explain the presence of the correlation of transcription levels of LADs with the probability to be near the NE, and the absence of any causal connection to transcription. In this picture, we assume that the state of being in affinity to the NE is set outside the interphase, at least outside of the G1 state that we model. Second, the NE may contain proteins that interact with gene-poor chromatin and define the epigenetic status of TADs by modifying their histone tails. In this mechanism, the initial postmitotic interaction of a chromatin locus with the NE proteins sets its "LAD status" for the rest of the interphase. These settings include accumulation of repressive epigenetic marks and frequent contacts with the NE during the interphase. Experimental support exists for both of these mechanisms (see Discussion).

We suggest that a lowering of transcriptional activities of L-TADs with the increase of their probability to be in contact with the NE (Fig. 2 (E)) is due to a combination of genetic content and chromatin features in L-TADs. This suggestion can be most relevant for the L-TADs in the two bins # 5 and # 6 of Fig. 2(E) with the probability to be in contact with the NE greater than 0.6.

A way to reconcile our general findings with the tethering experiments described above is to assume that the epigenetic state of a TAD can be reset by a contact with the lamina, but that reset requires a cell going through mitosis and forming a new NE, after which the locus has a relatively long and persistent contact with the NE. Likewise, once the epigenetic state is set, a long and persistent absence of the contact is needed for a return to the original state. Only a subset of TADs are liable to such a reset. The underlying assumption is that a relatively long time is needed to reset the epigenetic state, as appears to be the case in experiments where the epigenetic state is reset by a mechanical compression of the nucleus ***Wang et al.*** (***2017***).

Finally, we speculate that in early periods of eukaryotic nuclei evolution, lamina may have played a more direct role in the suppression of transcriptional activity. Due to initial evolutionary selection, genes with smaller desired levels of transcription may have been placed into the L-TADs, which were more frequently in contact with the NE. Later, the gene suppressing role of lamina was replaced by a more universal and complicated mechanism of gene regulation ***Leemans et al.*** (***2019***), which does not depend on being in contact with the lamina.

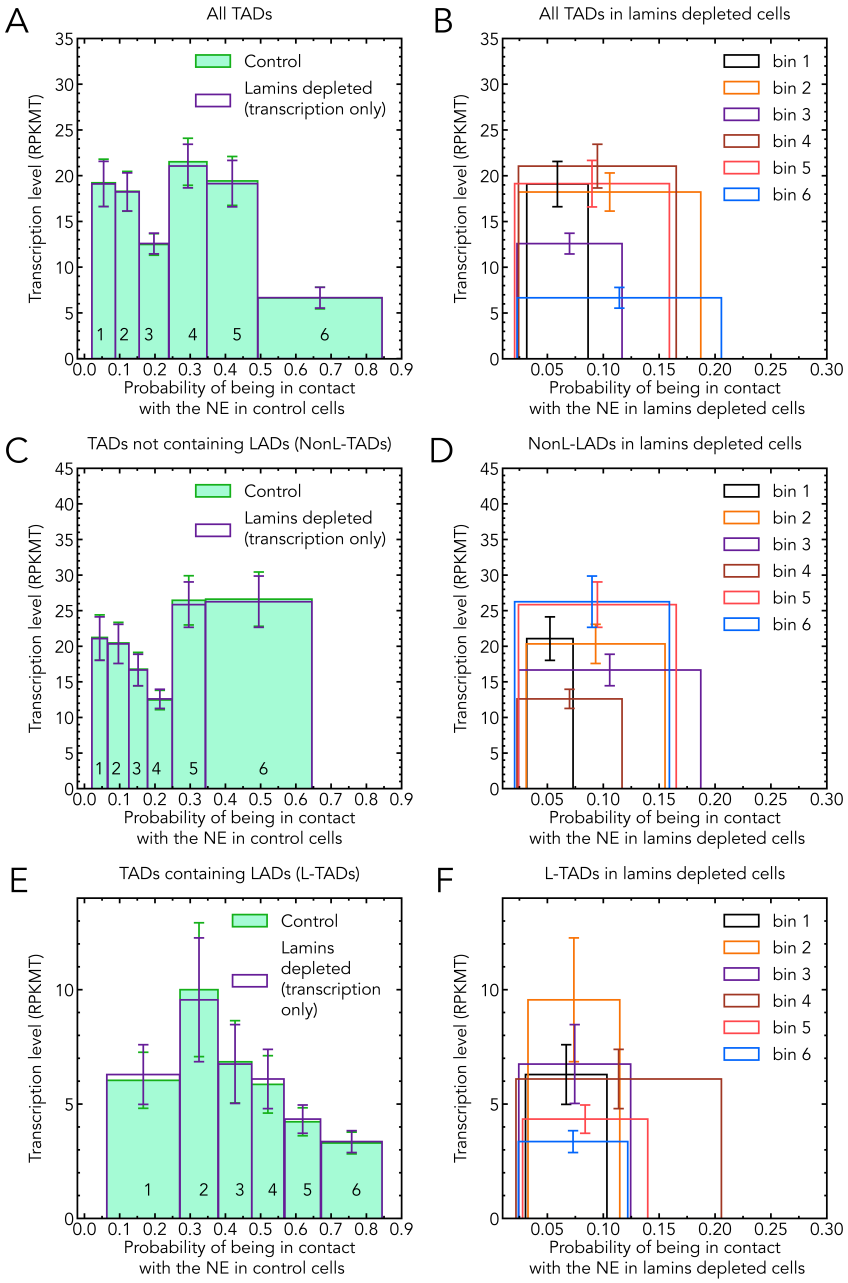

Figure 2. Dependencies of bin averaged TAD transcription levels (RPKMT) on the probabilities of TADs to be in contact with the NE. **Left column, solid bars: control cells. (A)** all TADs, **(C)** TADs not containing LADs (NonL-TADs), and **(E)** TADs containing LADs (L-TADs). Binning of TADs is based on TAD-NE contact probabilities in control cells for each set (selection) of TADs. The bin averaged TAD transcription levels (RPKMT) for lamins depleted cells for the same selection of TADs and bins are shown by empty bars in the same panels **(A)**, **(C)** and **(E)**. The positions of the bins along the x-axis is kept unchanged to facilitate visual comparison with the heights of the corresponding control bins. **Right column: lamins depleted cells.** Dependencies of bin averaged TAD transcription levels in lamins depleted cells on the probabilities of TADs to be in contact with the NE for lamins depleted cells are shown in panels **(B)**, **(D)** and **(F)** for all TADs, NonL-TADs and L-TADs, respectively, keeping the same binning as in the left set of panels. Error bars are s.e.m. (standard error of the mean).

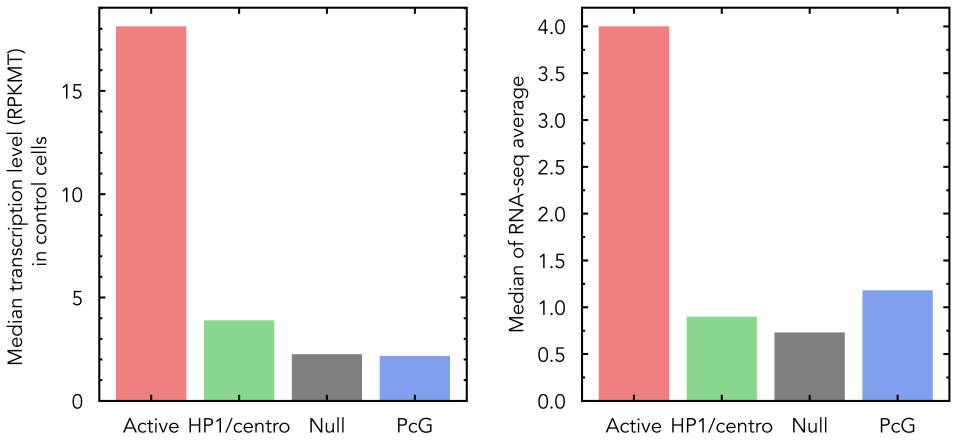

Figure 3. Median of transcription levels in Active TADs (in RPKMT) is much higher than those of other epigenetic TAD classes, such as HP1/centromeric, Null, and PcG **(left panel)**. The differences between the median transcription levels of non-Active classes are considerably smaller than the difference between the Active and non-Active TAD classes. These data are consistent with the data in Figure 3C of Ref. ***Sexton et al.*** (***2012***), reproduced in the **right panel**, which show the median of the gene transcription levels within each epigenetic class of TADs. The dynamic model of fruit fly nucleus employs the partitioning of genome into TADs and their epigenetic classes, introduced in Ref. ***Sexton et al.*** (***2012***).

Materials and Methods

Normalized measure of gene transcription levels at the TAD resolution

RNA-seq methods generate data that needs to be normalized to eliminate technical biases associated with the methods, such as the sequencing depth of a sample and the length of the mRNA transcripts ***Wagner et al.*** (***2012***). To correct these biases, RPKM (reads per kilobase of transcript per million reads mapped) measure has been widely used ***Wagner et al.*** (***2012***).

$$RPKM = \frac{10^9 \times \text{Reads mapped to transcript}}{\text{Total mapped reads} \times \text{Transcript length in bp}} \tag{1}$$

To quantify the average gene expression levels in a TAD, we propose a new metric, RPKMT (number of Reads mapped to all genes in a TAD Per Kilobase of TAD length per Million reads mapped to all TADs). This metric is similar to RPKM, but characterises all genes in a TAD, and the length of a TAD is used to normalize the number of reads to obtain the average transcription levels at TAD resolution.

$$RPKMT = \frac{10^9 \times \text{Reads mapped to genes in a TAD}}{\text{Total reads in all TADs} \times \text{TAD length in bp}} \tag{2}$$

We have verified that the proposed metric of transcription activity, Eq. 2, applied to the RNA-seq data from Ref. ***Ulianov et al.*** (***2019***), is consistent with the epigenetic classes of TADs identified previously ***Sexton et al.*** (***2012***), which are employed by our computational model. Specifically, we consider two transcription profiles to be consistent if their corresponding medians over TAD classes satisfy the following criteria simultaneously: (i) transcription level of Active TADs is much higher than those of all other epigenetic TAD classes and (ii) the differences between the transcription levels of non-Active classes are considerably smaller than the difference between the Active TADs and the other classes.

The consistency is demonstrated in Fig. 3. This consistency check mitigates potential concerns related to inevitable, but apparently minor, differences in gene expression profiles that may stem from differences between the types of embryonic cells from Ref. ***Ulianov et al.*** (***2019***) (S2 embryonic cell line) vs. those ***Sexton et al.*** (***2012***) (embryos collected 16-18 hour after egg laying) employed to build the computational model employed here. Another possible source of the observed

differences in gene expression profiles shown in Fig. 3, specifically a slightly higher ratio of Active to non-Active median TAD levels in our RPMKT based transcription profile (Fig. 3, left panel) compared to the profile from ***Sexton et al.*** (***2012***) (Fig. 3, right panel), may be related to the fact that, by construction, RPKMT metric is biased by the fraction of coding to non-coding DNA in a TAD.

Since RPKMT uses the total length of a TAD as its normalization factor, regardless of numbers of regions belonged to genes, RPKMT characterizes the transcription reads densities based on the actual length of TADs in chromatin.

Calculation of RPKMT from published RNA-seq data

The RNA-seq data used here contains two replicates (rep # 1 and rep # 2) of control S2 cells (samples GSM3449348 and GSM3449349) or lamins depleted cells (samples GSM3449350 and GSM3449351) ***Ulianov et al.*** (***2019***). Genes are assigned to a TAD if their transcription start sites are located within the TAD, according to BDGP Release 5/dm3 ***Fujita et al.*** (***2011***). The transcription activity metric, equation 2 is the calculated as:

$$RPKMT = \frac{10^9 \times (\text{Reads of rep \# 1 and rep \# 2 mapped to genes in a TAD})}{(\text{Total reads of rep \# 1 and rep \# 2 in all TADs}) \times \text{TAD length in bp}} \quad (3)$$

The dynamic model of interphase chromosomes at TAD resolution

To determine the probabilities of TADs to be in contact with the NE, we use a dynamic model of a *D.melanogaster* female interphase nucleus with a diploid set of four homologous chromosomes, developed in our previous work ***Tolokh et al.*** (***2022***). A brief description of the model is given below.

The model simulates the dynamics of the chromatin fibers for a time equivalent to 11 hours, the duration of the *D.melanogaster* nucleus interphase, and allows analyzing the trajectories of individual TADs in both control and lamins depleted (LD) nuclei.

In the model, each pair of homologous chromosomes (2, 3, 4 and X), which are in proximity to each other ***Fung et al.*** (***1998***), is represented by a single chain of spherical beads using the bead-spring model ***Lifshitz et al.*** (***1978***); ***Mirny*** (***2011***). The four chains of these beads are surrounded by a spherical boundary representing the NE. 1169 beads in these chains correspond to 1169 pairs of homologous TADs - physical domains resolved in the Hi-C maps ***Sexton et al.*** (***2012***). Additionally, 4 beads represent centromeric chromatin domains (CEN) in each chain, and 6 beads adjacent to CEN beads represent pericentromeric constitutive heterochromatin domains (HET). The mass and the size of each bead corresponds to the length of the DNA contained in the corresponding TAD, CEN or HET domains.

The model employs four well-established, major classes of TADs (Active, Null, PcG, and HP1) identified previously ***Sexton et al.*** (***2012***) based on their epigenetic signatures ***Filion et al.*** (***2010***) and biological functions. Following bead–TAD equivalence in the model, it has four corresponding bead types. Each bead/TAD type is characterized by its own interaction well depth parameter ϵ_t for attractive interactions between beads of the same type. Interactions between beads of different types are not type-specific and are characterized by a single well depth parameter ϵ_g. The beads corresponding to TADs that contain lamina associated domains (LADs) ***Pickersgill et al.*** (***2006***); ***van Bemmel et al.*** (***2010***) – L-TADs – can attractively interact with the NE. This L-TAD–NE affinity can temporally confine L-TADs at the NE. The interaction parameters of the model are tuned to reproduce: (i) the average experimental fraction of LADs confined to the NE, 25% ***Pickersgill et al.*** (***2006***) and (ii) the experimental TAD-TAD contact probability (Hi-C) map ***Sexton et al.*** (***2012***); ***Li et al.*** (***2017***) (Pearson's correlation coefficient is 0.956). The model predicts highly dynamical distributions of the chromatin (both for control and LD nuclei), which, after averaging, are in a good agreement with the experimentally observed average density profiles of fruit fly chromatin ***Bondarenko and Sharakhov*** (***2020***). As in the experiment, the chromatin density distribution in the model LD nuclei shows a substantial shift of the chromatin from the NE, compared to the distribution in control nuclei, accompanied by a large increase of the density in the central nucleus region (see Fig. 1 in Appendix 2).

The model also correctly reproduces the experimentally observed change of average radial positioning of individual cytological regions (22A, 36C and 60D) explored previously ***Ulianov et al.*** (***2019***) in the LD nuclei (see Fig. 2 in Appendix 1).

Binning of the TAD transcription data based on contact with NE probabilities

The TADs are grouped into six bins, according to the probability of each TAD to be in contact with the NE in control cells. For 1169 TADs, Figure 2 (A and B), bins # 1-5 contain 194 elements each, whereas bin # 6 has 195 elements. For 350 L-TADs, Figure 2 (C and D), bins # 1-5 contain 58 elements each, whereas bin # 6 has 60 elements. For 819 nonL-TADs, Figure 2 (E and F), bins # 1-5 contain 137 elements each, whereas bin # 6 has 134 elements. The number of bins is determined by a reasonable balance between two opposing requirements: enough bins are needed to clearly identify a trend in transcription level changes, but too many bins result in higher standard error of the mean transcription level per bin.

Acknowledgments

This research was supported by the National Science Foundation (MCB-1715207). We thank Raju Nadimpalli and team members.

References

Acemel RD, Maeso I, Gómez-Skarmeta JL. Topologically associated domains: a successful scaffold for the evolution of gene regulation in animals. WIREs Developmental Biology. 2017 Mar; 6(3). https://doi.org/10.1002/wdev.265, doi: 10.1002/wdev.265.

Amiad-Pavlov D, Lorber D, Bajpai G, Reuveny A, Roncato F, Alon R, Safran S, Volk T. Live imaging of chromatin distribution reveals novel principles of nuclear architecture and chromatin compartmentalization. Science Advances. 2021 Jun; 7(23). https://doi.org/10.1126/sciadv.abf6251, doi: 10.1126/sciadv.abf6251.

van Bemmel JG, Pagie L, Braunschweig U, Brugman W, Meuleman W, Kerkhoven RM, van Steensel B. The Insulator Protein SU(HW) Fine-Tunes Nuclear Lamina Interactions of the Drosophila Genome. PLoS ONE. 2010 Nov; 5(11):e15013. https://doi.org/10.1371/journal.pone.0015013, doi: 10.1371/journal.pone.0015013.

Bondarenko SM, Sharakhov IV. Reorganization of the nuclear architecture in the Drosophila melanogaster Lamin B mutant lacking the CaaX box. Nucleus. 2020 Jan; 11(1):283–298. https://doi.org/10.1080/19491034.2020.1819704, doi: 10.1080/19491034.2020.1819704.

Briand N, Collas P. Lamina-associated domains: peripheral matters and internal affairs. Genome Biology. 2020 Apr; 21(1). https://doi.org/10.1186/s13059-020-02003-5, doi: 10.1186/s13059-020-02003-5.

Buchwalter A, Kaneshiro JM, Hetzer MW. Coaching from the sidelines: the nuclear periphery in genome regulation. Nature Reviews Genetics. 2018 Oct; 20(1):39–50. https://doi.org/10.1038/s41576-018-0063-5, doi: 10.1038/s41576-018-0063-5.

Chuang CH, Carpenter AE, Fuchsova B, Johnson T, de Lanerolle P, Belmont AS. Long-Range Directional Movement of an Interphase Chromosome Site. Current Biology. 2006 Apr; 16(8):825–831. https://doi.org/10.1016/j.cub.2006.03.059, doi: 10.1016/j.cub.2006.03.059.

Chubb JR, Boyle S, Perry P, Bickmore WA. Chromatin Motion Is Constrained by Association with Nuclear Compartments in Human Cells. Current Biology. 2002 Mar; 12(6):439–445. https://doi.org/10.1016/s0960-9822(02)00695-4, doi: 10.1016/s0960-9822(02)00695-4.

Csink AK, Henikoff S. Large-scale Chromosomal Movements During Interphase Progression in Drosophila. Journal of Cell Biology. 1998 10; 143(1):13–22. https://doi.org/10.1083/jcb.143.1.13, doi: 10.1083/jcb.143.1.13.

Demmerle J, Koch AJ, Holaska JM. Emerin and histone deacetylase 3 (HDAC3) cooperatively regulate expression and nuclear positions of MyoD, Myf5, and Pax7 genes during myogenesis. Chromosome Research. 2013 Sep; 21(8):765–779. https://doi.org/10.1007/s10577-013-9381-9, doi: 10.1007/s10577-013-9381-9.

Dietzel S, Zolghadr K, Hepperger C, Belmont AS. Differential large-scale chromatin compaction and intranuclear positioning of transcribed versus non-transcribed transgene arrays containing β - globin regulatory sequences. Journal of Cell Science. 2004; 117(19):4603–4614. https://journals.biologists.com/jcs/article/117/19/4603/27803/Differential-large-scale-chromatin-compaction-and, doi: https://doi.org/10.1242/jcs.01330.

Dixon JR, Jung I, Selvaraj S, Shen Y, Antosiewicz-Bourget JE, Lee AY, Ye Z, Kim A, Rajagopal N, Xie W, Diao Y, Liang J, Zhao H, Lobanenkov VV, Ecker JR, Thomson JA, Ren B. Chromatin architecture reorganization during stem cell differentiation. Nature. 2015 Feb; 518(7539):331–336. https://doi.org/10.1038/nature14222, doi: 10.1038/nature14222.

Dixon JR, Selvaraj S, Yue F, Kim A, Li Y, Shen Y, Hu M, Liu JS, Ren B. Topological domains in mammalian genomes identified by analysis of chromatin interactions. Nature. 2012 Apr; 485(7398):376–380. https://doi.org/10.1038/nature11082, doi: 10.1038/nature11082.

Filion G, Van Bemmel J, Braunschweig U, Talhout W, Kind J, Ward L, Brugman W, Castro I, Kerkhoven R, Bussemaker H, van Steensel B. Systematic Protein Location Mapping Reveals Five Principal Chromatin Types in Drosophila Cells. Cell. 2010 09; 143:212–24. doi: 10.1016/j.cell.2010.09.009.

Finlan LE, Sproul D, Thomson I, Boyle S, Kerr E, Perry P, Ylstra B, Chubb JR, Bickmore WA. Recruitment to the Nuclear Periphery Can Alter Expression of Genes in Human Cells. PLOS Genetics. 2008; 4:1–13. https://doi.org/10.1371/journal.pgen.1000039, doi: 10.1371/journal.pgen.1000039.

Fujita PA, Rhead B, Zweig AS, Hinrichs AS, Karolchik D, Cline MS, Goldman M, Barber GP, Clawson H, Coelho A, Diekhans M, Dreszer TR, Giardine BM, Harte RA, Hillman-Jackson J, Hsu F, Kirkup V, Kuhn RM, Learned K, Li CH, et al. The UCSC Genome Browser database: update 2011. Nucleic Acids Research. 2011 Oct; 39(Database):D876–D882. https://doi.org/10.1093/nar/gkq963, doi: 10.1093/nar/gkq963.

Fung JC, Marshall WF, Dernburg A, Agard DA, Sedat JW. Homologous Chromosome Pairing in Drosophila melanogaster Proceeds through Multiple Independent Initiations. Journal of Cell Biology. 1998 Apr; 141(1):5–20. https://doi.org/10.1083/jcb.141.1.5, doi: 10.1083/jcb.141.1.5.

Gorkin DU, Leung D, Ren B. The 3D Genome in Transcriptional Regulation and Pluripotency. Cell Stem Cell. 2014 Jun; 14(6):762–775. https://doi.org/10.1016/j.stem.2014.05.017, doi: 10.1016/j.stem.2014.05.017.

Guelen L, Pagie L, Brasset E, Meuleman W, Faza MB, Talhout W, Eussen BH, de Klein A, Wessels L, de Laat W, van Steensel B. Domain organization of human chromosomes revealed by mapping of nuclear lamina interactions. Nature. 2008 May; 453(7197):948–951. https://doi.org/10.1038/nature06947, doi: 10.1038/nature06947.

Hewitt SL, High FA, Reiner SL, Fisher AG, Merkenschlager M. Nuclear repositioning marks the selective exclusion of lineage-inappropriate transcription factor loci during T helper cell differentiation. European journal of immunology. 2004; 34:3604–13. https://pubmed.ncbi.nlm.nih.gov/15484194/, doi: 10.1002/eji.200425469.

Kim Y, Zheng X, Zheng Y. Role of lamins in 3D genome organization and global gene expression. Nucleus. 2019 Jan; 10(1):33–41. https://doi.org/10.1080/19491034.2019.1578601, doi: 10.1080/19491034.2019.1578601.

Kind J, Pagie L, Ortabozkoyun H, Boyle S, de Vries SS, Janssen H, Amendola M, Nolen LD, Bickmore WA, van Steensel B. Single-Cell Dynamics of Genome-Nuclear Lamina Interactions. Cell. 2013 Mar; 153(1):178–192. https://doi.org/10.1016/j.cell.2013.02.028, doi: 10.1016/j.cell.2013.02.028.

Kind J, Pagie L, de Vries SS, Nahidiazar L, Dey SS, Bienko M, Zhan Y, Lajoie B, de Graaf CA, Amendola M, Fudenberg G, Imakaev M, Mirny LA, Jalink K, Dekker J, van Oudenaarden A, van Steensel B. Genome-wide Maps of Nuclear Lamina Interactions in Single Human Cells. Cell. 2015 Sep; 163(1):134–147. https://doi.org/10.1016/j.cell.2015.08.040, doi: 10.1016/j.cell.2015.08.040.

Kosak ST, Medina JASKL, Riblet R, Beau MML, Fisher AG, Singh H. Subnuclear Compartmentalization of Immunoglobulin Loci During Lymphocyte Development. Science. 2002; 296:158–162. https://www.science.org/doi/full/10.1126/science.1068768, doi: 10.1126/science.1068768.

Kumaran RI, Spector DL. A genetic locus targeted to the nuclear periphery in living cells maintains its transcriptional competence. Journal of Cell Biology. 2008 Jan; 180(1):51–65. https://doi.org/10.1083/jcb.200706060, doi: 10.1083/jcb.200706060.

Lanctôt C, Cheutin T, Cremer M, Cavalli G, Cremer T. Dynamic genome architecture in the nuclear space: regulation of gene expression in three dimensions. Nature Reviews Genetics. 2007 Feb; 8(2):104–115. https://doi.org/10.1038/nrg2041, doi: 10.1038/nrg2041.

Lee DC, Welton KL, Smith ED, Kennedy BK. A-type nuclear lamins act as transcriptional repressors when targeted to promoters. Experimental Cell Research. 2009 Apr; 315(6):996–1007. https://doi.org/10.1016/j.yexcr.2009.01.003, doi: 10.1016/j.yexcr.2009.01.003.

Leemans C, van der Zwalm MCH, Brueckner L, Comoglio F, van Schaik T, Pagie L, van Arensbergen J, van Steensel B. Promoter-Intrinsic and Local Chromatin Features Determine Gene Repression in LADs. Cell. 2019; 177(4):852–864.e14. https://www.sciencedirect.com/science/article/pii/S0092867419302715, doi: https://doi.org/10.1016/j.cell.2019.03.009.

Li Q, Tjong H, Li X, Gong K, Zhou XJ, Chiolo I, Alber F. The three-dimensional genome organization of Drosophila melanogaster through data integration. Genome Biology. 2017 Jul; 18(1). https://doi.org/10.1186/s13059-017-1264-5, doi: 10.1186/s13059-017-1264-5.

Liao Y, Zhang X, Chakraborty M, Emerson JJ. Topologically associating domains and their role in the evolution of genome structure and function in Drosophila. Genome Research. 2021; 31(3):397–410. http://genome.cshlp.org/content/31/3/397.abstract, doi: 10.1101/gr.266130.120.

Lieberman-Aiden E, van Berkum NL, Williams L, Imakaev M, Ragoczy T, Telling A, Amit I, Lajoie BR, Sabo PJ, Dorschner MO, Sandstrom R, Bernstein B, Bender MA, Groudine M, Gnirke A, Stamatoyannopoulos J, Mirny LA, Lander ES, Dekker J. Comprehensive Mapping of Long-Range Interactions Reveals Folding Principles of the Human Genome. Science. 2009 Oct; 326(5950):289–293. https://doi.org/10.1126/science.1181369, doi: 10.1126/science.1181369.

Lifshitz IM, Grosberg AY, Khokhlov AR. Some problems of the statistical physics of polymer chains with volume interaction. Rev Mod Phys. 1978 Jul; 50:683–713. https://link.aps.org/doi/10.1103/RevModPhys.50.683, doi: 10.1103/RevModPhys.50.683.

Malhas A, Lee CF, Sanders R, Saunders NJ, Vaux DJ. Defects in lamin B1 expression or processing affect interphase chromosome position and gene expression. The Journal of cell biology. 2007; 176:593–603. https://rupress.org/jcb/article/176/5/593/34512/Defects-in-lamin-B1-expression-or-processing, doi: 10.1083/jcb.200607054.

Metsalu T, Vilo J. ClustVis: a web tool for visualizing clustering of multivariate data using Principal Component Analysis and heatmap. Nucleic Acids Research. 2015 05; 43(W1):W566–W570. https://doi.org/10.1093/nar/gkv468, doi: 10.1093/nar/gkv468.

Milon BC, Cheng H, Tselebrovsky MV, Lavrov SA, Nenasheva VV, Mikhaleva EA, Shevelyov YY, Nurminsky DI. Role of Histone Deacetylases in Gene Regulation at Nuclear Lamina. PLoS ONE. 2012 Nov; 7(11):e49692. https://doi.org/10.1371/journal.pone.0049692, doi: 10.1371/journal.pone.0049692.

Mirny LA. The fractal globule as a model of chromatin architecture in the cell. Chromosome Research. 2011 Jan; 19(1):37–51. https://doi.org/10.1007/s10577-010-9177-0, doi: 10.1007/s10577-010-9177-0.

Misteli T. Beyond the sequence: cellular organization of genome function. Cell. 2007; 128(4):787–800. https://pubmed.ncbi.nlm.nih.gov/17320514/, doi: 10.1016/j.cell.2007.01.028.

Nielsen JA, Hudson LD, Armstrong RC. Nuclear organization in differentiating oligodendrocytes. Journal of Cell Science. 2002; 115:4071–4079. https://journals.biologists.com/jcs/article/115/21/4071/34916/Nuclear-organization-in-differentiating, doi: 10.1242/jcs.00103.

Nora EP, Lajoie BR, Schulz EG, Giorgetti L, Okamoto I, Servant N, Piolot T, van Berkum NL, Meisig J, Sedat J, Gribnau J, Barillot E, Blüthgen N, Dekker J, Heard E. Spatial partitioning of the regulatory landscape of the X-inactivation centre. Nature. 2012 Apr; 485(7398):381–385. https://doi.org/10.1038/nature11049, doi: 10.1038/nature11049.

Phillips-Cremins JE, Sauria MEG, Sanyal A, Gerasimova TI, Lajoie BR, Bell JSK, Ong CT, Hookway TA, Guo C, Sun Y, Bland MJ, Wagstaff W, Dalton S, McDevitt TC, Sen R, Dekker J, Taylor J, Corces VG. Architectural Protein Subclasses Shape 3D Organization of Genomes during Lineage Commitment. Cell. 2013 Jun; 153(6):1281–1295. https://doi.org/10.1016/j.cell.2013.04.053, doi: 10.1016/j.cell.2013.04.053.

Pickersgill H, Kalverda B, de Wit E, Talhout W, Fornerod M, van Steensel B. Characterization of the Drosophila melanogaster genome at the nuclear lamina. Nature Genetics. 2006 Jul; 38(9):1005–1014. https://doi.org/10.1038/ng1852, doi: 10.1038/ng1852.

Pindyurin AV, Ilyin AA, Ivankin AV, Tselebrovsky MV, Nenasheva VV, Mikhaleva EA, Pagie L, van Steensel B, , Shevelyov YY. The large fraction of heterochromatin in Drosophila neurons is bound by both B-type lamin and HP1a. Epigenetics Chromatin. 2018; 11(65):17 pages. https://doi.org/10.1186/s13072-018-0235-8, doi: 10.1186/s13072-018-0235-8.

Poleshko A, Shah PP, Gupta M, Babu A, Morley MP, Manderfield LJ, Ifkovits JL, Calderon D, Aghajanian H, Sierra-Pagán JE, Sun Z, Wang Q, Li L, Dubois NC, Morrisey EE, Lazar MA, Smith CL, Epstein JA, Jain R. Genome-Nuclear Lamina Interactions Regulate Cardiac Stem Cell Lineage Restriction. Cell. 2017 Oct; 171(3):573–587.e14. https://doi.org/10.1016/j.cell.2017.09.018, doi: 10.1016/j.cell.2017.09.018.

Rao SSP, Huntley MH, Durand NC, Stamenova EK, Bochkov ID, Robinson JT, Sanborn AL, Machol I, Omer AD, Lander ES, Aiden EL. A 3D Map of the Human Genome at Kilobase Resolution Reveals Principles of Chromatin Looping. Cell. 2014 Dec; 159(7):1665–1680. https://doi.org/10.1016/j.cell.2014.11.021, doi: 10.1016/j.cell.2014.11.021.

Reddy KL, Zullo JM, Bertolino E, Singh H. Transcriptional repression mediated by repositioning of genes to the nuclear lamina. Nature. 2008; 452:243–247. https://doi.org/10.1038/nature06727, doi: 10.1038/nature06727.

Renschler G, Richard G, Valsecchi CIK, Toscano S, Arrigoni L, Ramírez F, Akhtar A. Hi-C guided assemblies reveal conserved regulatory topologies on X and autosomes despite extensive genome shuffling. Genes & Development. 2019 Oct; 33(21-22):1591–1612. https://doi.org/10.1101/gad.328971.119, doi: 10.1101/gad.328971.119.

Rowley MJ, Corces VG. Organizational principles of 3D genome architecture. Nature Reviews Genetics. 2018 Oct; 19(12):789–800. https://doi.org/10.1038/s41576-018-0060-8, doi: 10.1038/s41576-018-0060-8.

Sexton T, Cavalli G. The Role of Chromosome Domains in Shaping the Functional Genome. Cell. 2015 Mar; 160(6):1049–1059. https://doi.org/10.1016/j.cell.2015.02.040, doi: 10.1016/j.cell.2015.02.040.

Sexton T, Yaffe E, Kenigsberg E, Bantignies F, Leblanc B, Hoichman M, Parrinello H, Tanay A, Cavalli G. Three-Dimensional Folding and Functional Organization Principles of the Drosophila Genome. Cell. 2012 Feb; 148(3):458–472. https://doi.org/10.1016/j.cell.2012.01.010, doi: 10.1016/j.cell.2012.01.010.

Shachar S, Misteli T. Causes and consequences of nuclear gene positioning. Journal of Cell Science. 2017 05; 130(9):1501–1508. https://doi.org/10.1242/jcs.199786, doi: 10.1242/jcs.199786.

Somech R, Shaklai S, Geller O, Amariglio N, Simon AJ, Rechavi G, Gal-Yam EN. The nuclear-envelope protein and transcriptional repressor LAP2beta interacts with HDAC at the nuclear periphery, and induces histone H4 deacetylation. Journal of Cell Science. 2005 Sep; 118(17):4017–4025. https://doi.org/10.1242/jcs.02521, doi: 10.1242/jcs.02521.

Spector DL. The Dynamics of Chromosome Organization and Gene Regulation. Annual Review of Biochemistry. 2003; 72(1):573–608. doi: 10.1146/annurev.biochem.72.121801.161724.

Stephens AD, Liu PZ, Banigan EJ, Almassalha LM, Backman V, Adam SA, Goldman RD, Marko JF. Chromatin histone modifications and rigidity affect nuclear morphology independent of lamins. Molecular Biology of the Cell. 2018 Jan; 29(2):220–233. https://doi.org/10.1091/mbc.e17-06-0410, doi: 10.1091/mbc.e17-06-0410.

Tolokh IS, Kinney NA, Sharakhov IV, Onufriev AV. Strong interactions between highly-dynamic lamina-associated domains and the nuclear envelope stabilize the 3D architecture of Drosophila interphase chromatin. BioRxiv. 2022 Jan; https://www.biorxiv.org/content/10.1101/2022.01.28.478236v1, doi: 10.1101/2022.01.28.478236.

Torosin NS, Anand A, Golla TR, Cao W, Ellison CE. 3D genome evolution and reorganization in the Drosophila melanogaster species group. PLOS Genetics. 2020 Dec; 16(12):e1009229. https://doi.org/10.1371/journal.pgen.1009229, doi: 10.1371/journal.pgen.1009229.

Ulianov SV, Doronin SA, Khrameeva EE, Kos PI, Luzhin AV, Starikov SS, Galitsyna AA, Nevasheva VV, Ilyin AA, Flayamer IM, Mikhaleva EA, Logacheva MD, Gelfand MS, Chertovich AV, Gavrilov AA, Razin SV, Sheveloyov YY. Nuclear lamina integrity is required for proper spatial organization of chromatin in Drosophila. Nat Commun. 2019; 10. doi: https://doi.org/10.1038/s41467-019-09185-y.

Ulianov SV, Khrameeva EE, Gavrilov AA, Flyamer IM, Kos P, Mikhaleva EA, Penin AA, Logacheva MD, Imakaev MV, Chertovich A, Gelfand MS, Shevelyov YY, Razin SV. Active chromatin and transcription play a key role in chromosome partitioning into topologically associating domains. Genome Research. 2015 Oct; 26(1):70–84. https://doi.org/10.1101/gr.196006.115, doi: 10.1101/gr.196006.115.

Ulianov SV, Zakharova VV, Galitsyna AA, Kos PI, Polovnikov KE, Flyamer IM, Mikhaleva EA, Khrameeva EE, Germini D, Logacheva MD, Gavrilov AA, Gorsky AS, Nechaev SK, Gelfand MS, Vassetzky YS, Chertovich AV, Shevelyov YY, Razin SV. Order and stochasticity in the folding of individual Drosophila genomes. Nature Communications. 2021 Jan; 12(1). https://doi.org/10.1038/s41467-020-20292-z, doi: 10.1038/s41467-020-20292-z.

Wagner GP, Kin K, Lynch VJ. Measurement of mRNA abundance using RNA-seq data: RPKM measure is inconsistent among samples. Theory in Biosciences. 2012 Aug; 131(4):281–285. https://doi.org/10.1007/s12064-012-0162-3, doi: 10.1007/s12064-012-0162-3.

Wang Y, Nagarajan M, Uhler C, Shivashankar GV. Orientation and repositioning of chromosomes correlate with cell geometry–dependent gene expression. Molecular Biology of the Cell. 2017 Jul; 28(14):1997–2009. https://doi.org/10.1091/mbc.e16-12-0825, doi: 10.1091/mbc.e16-12-0825.

Williams RRE, Azuara V, Perry P, Sauer S, Dvorkina M, Jørgensen H, Roix J, McQueen P, Misteli T, Merkenschlager M, Fisher AG. Neural induction promotes large-scale chromatin reorganisation of the Mash1 locus. The Journal of cell biology. 2006; 119:132–140. https://journals.biologists.com/jcs/article/119/1/132/28781/Neural-induction-promotes-large-scale-chromatin, doi: 10.1242/jcs.02727.

Wu F, Yao J. Identifying Novel Transcriptional and Epigenetic Features of Nuclear Lamina-associated Genes. Scientific Reports. 2017 Mar; 7(1). https://doi.org/10.1038/s41598-017-00176-x, doi: 10.1038/s41598-017-00176-x.

Yasuhara T, Zou L. Impacts of chromatin dynamics and compartmentalization on DNA repair. DNA Repair. 2021 Sep; 105:103162. https://doi.org/10.1016/j.dnarep.2021.103162, doi: 10.1016/j.dnarep.2021.103162.

Zheng X, Kim Y, Zheng Y. Identification of lamin B–regulated chromatin regions based on chromatin landscapes. Molecular Biology of the Cell. 2015 Jul; 26(14):2685–2697. https://doi.org/10.1091/mbc.e15-04-0210, doi: 10.1091/mbc.e15-04-0210.

Zhou J, Ermakova OV, Riblet R, Birshtein BK, Schildkraut CL. Replication and Subnuclear Location Dynamics of the Immunoglobulin Heavy-Chain Locus in B-Lineage Cells. Molecular and Cellular Biology. 2002; 22:4876–4889. https://doi.org/10.1128/MCB.22.13.4876-4889.2002, doi: 10.1128/MCB.22.13.4876-4889.2002.

Zink D, Amaral MD, Englmann A, Lang S, Clarke LA, Rudolph C, Alt F, Luther K, Braz C, Sadoni N, Rosenecker J, Schindelhauer D. Transcription-dependent spatial arrangements of CFTR and adjacent genes in human cell nuclei. Journal of Cell Biology. 2004 Sep; 166(6):815–825. https://doi.org/10.1083/jcb.200404107, doi: 10.1083/jcb.200404107.

Zullo JM, Demarco IA, Piqué-Regi R, Gaffney DJ, Epstein CB, Spooner CJ, Luperchio TR, Bernstein BE, Pritchard JK, Reddy KL, Singh H. DNA Sequence-Dependent Compartmentalization and Silencing of Chromatin at the Nuclear Lamina. Cell. 2012 Jun; 149(7):1474–1487. https://doi.org/10.1016/j.cell.2012.04.035, doi: 10.1016/j.cell.2012.04.035.

Appendix 1

To explain why mean RPKMT values are relatively low in bin # 3 and bin # 4 of NonL-TADs (Fig. 2 (C)) main text, we analyzed epigenetic marks in all six bins corresponding to the probabilities of NonL-TADs being in contact with the NE. As shown in Fig. 1 in Appendix 1, bin # 3 and bin # 4 (relatively low mean RPKMT values) are enriched in repressive epigenetic marks, whereas bin # 5 and bin # 6 (relatively high mean RPKMT values) are enriched in active epigenetic marks.

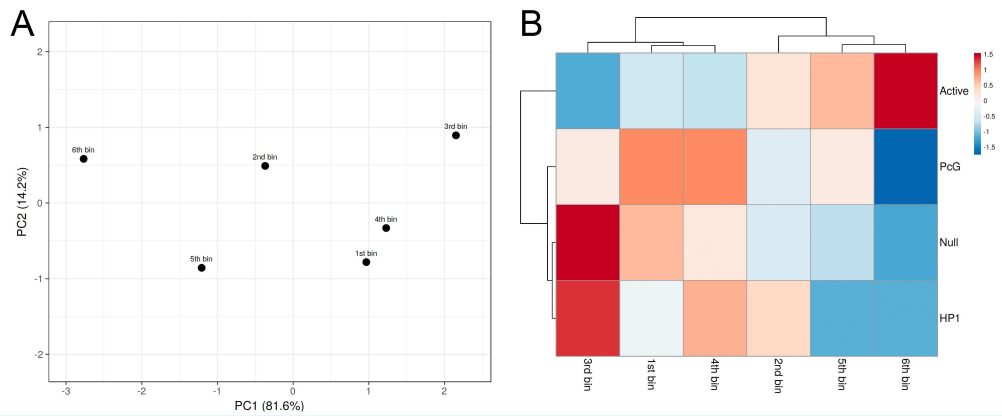

Appendix 1 Figure 1. Differences in epigenetic marks among 6 bins, corresponding to the probabilities of NonL-TADs to be in contact with the NE. **(A)** The PCA analysis showing that bin # 3 and bin # 4 (relatively low mean RPKMT values) are spatially separated from bin # 5 and bin # 6 (relatively high mean RPKMT values). **(B)** The heatmap showing that bin # 3 and bin # 4 (realtively low mean RPKMT values) are enriched in Null and HP1 nonL-TADs and in Null and PcG nonL-TADs, respectively. Bin # 5 and bin # 6 (relatively high mean RPKMT values) are enriched in active nonL-TADs. The PCA analysis was done using the online tool ClustVis (https://biit.cs.ut.ee/clustvis/) ***Metsalu and Vilo* (*2015*)**

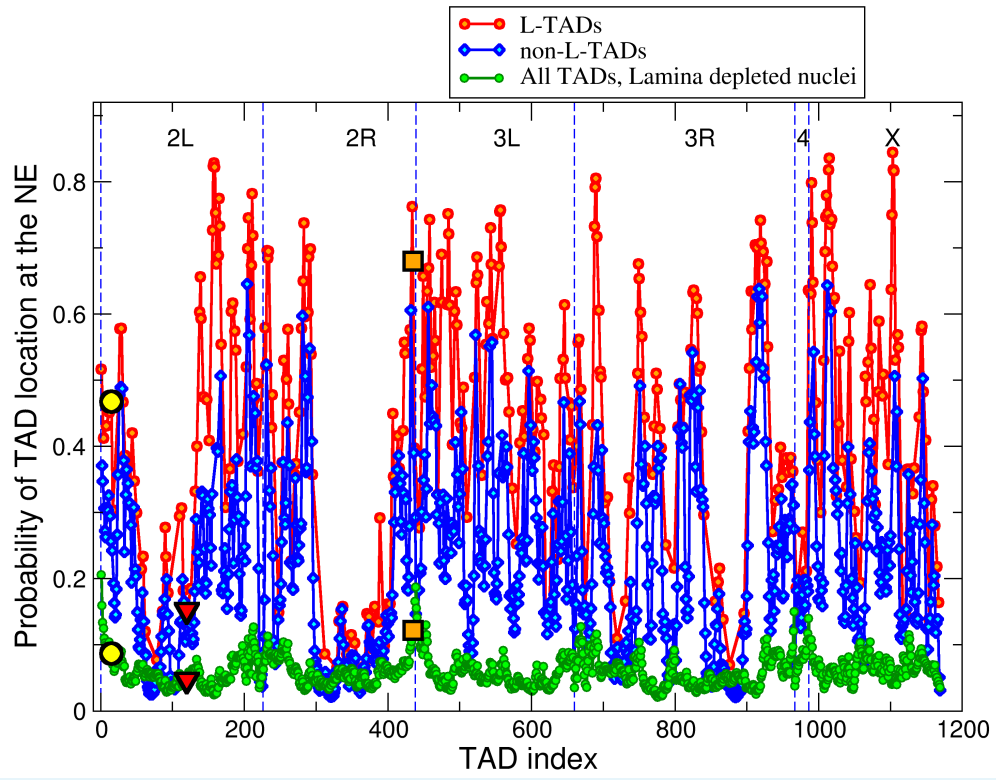

Appendix 1 Figure 2. Probabilities of TADs (LAD containing TADs (L-TADs) and TADs not containing LADs (nonL-TADs) in control nucleus model, and all TADs in lamins depleted (LD) nucleus model) to be in contact with the NE (to be within 0.2 μm from the NE). Null L-TADs #15 (for control and LD nuclei), analyzed in ***Ulianov et al.*** (***2019***) as cytological region $22A$, are marked by yellow circles. Null L-TADs #120 (for control and LD nuclei), analyzed in ***Ulianov et al.*** (***2019***) as cytological region $36C$, are marked by red triangles. PcG L-TADs #435 (for control and LD nuclei), analyzed in ***Ulianov et al.*** (***2019***) as cytological region $60D$, are marked by orange squares.

Appendix 2

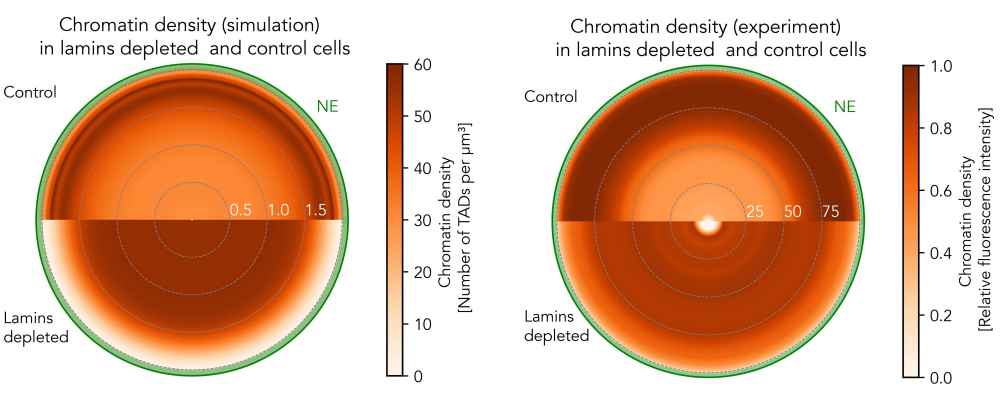

Appendix 2 Figure 1. Left panel: Computed chromatin density averaged over the spherical layers as a function of the radial distance from the nucleus center in control nuclei (top) and in lamins depleted nuclei (bottom). The radius of the nucleus is 2 μm. **Right panel**: Experimental mean chromatin radial density in the equatorial plane of the nucleus. For illustration only, the azimuthal dependence of the density is averaged out to produce a schematic that shows only the radial density profile. The density is inferred from relative fluorescence intensity, as detailed in Ref. ***Bondarenko and Sharakhov* (*2020*)**. Specifically, 21 equally spaced experimental data points are taken from Fig. S3 (Group 1, bottom panel) of Ref. ***Bondarenko and Sharakhov* (*2020*)** and then interpolated using a linear interpolation process, yielding 201 equally spaced data points plotted in the figure. The radial position of the mean chromatin density is measured from the nuclear center to the periphery (0 % - 100 %).

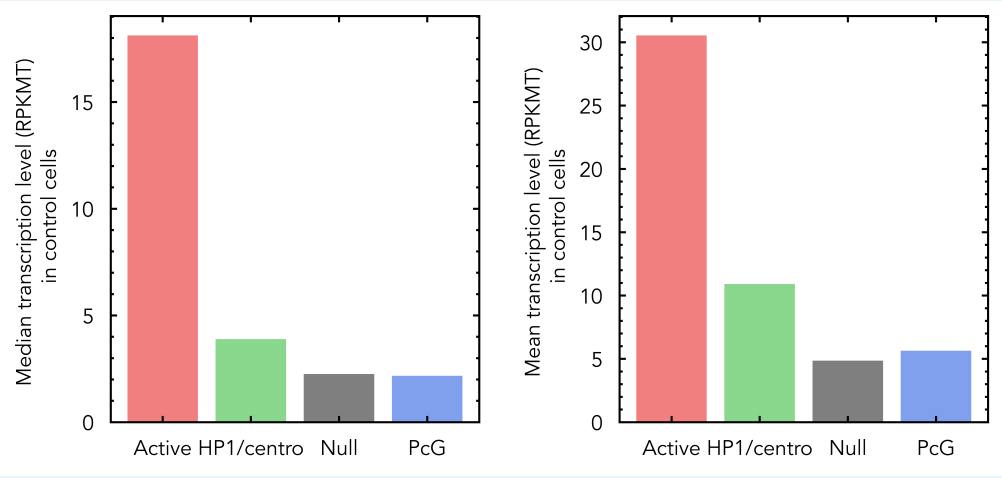

Appendix 2 Figure 2. Median (left) and mean (right) transcription levels in different epigenetic classes of TADs (in RPKMT). The consistency of RPKMT metric with the transcription level data (Fig.3 (right) in the main text), is demonstrated by the fact that the transcription levels (both median and mean) of Active TADs are much higher than those of other epigenetic TAD classes.